J. Fluid Mech. (1977), *vol.* 80, *part* 1, *pp.* 129–148
Printed in Great Britain

Laser light-scattering measurements of particle concentration in a turbulent jet

By E. J. SHAUGHNESSY

Department of Mechanical Engineering and Materials Science,
Duke University, Durham, North Carolina 27706

AND J. B. MORTON

Department of Engineering Science and Systems, University of Virginia,
Charlottesville

(Received 15 October 1975 and in revised form 24 March 1976)

A laser light-scattering technique has been used to study the relative particle concentration field in a round turbulent air jet. Measurements were made in the far field of a smoke-marked turbulent jet exhausting into a secondary air stream. Radial distributions of mean particle concentration, concentration fluctuation intensity and intermittency were measured at several streamwise locations. Concentration fluctuation power spectra and the micro- and integral scales of the concentration fluctuations were measured on the jet axis. The effects of ambiguity noise and noise due to optical path attenuation on the performance of the laser light-scattering system are discussed.

1. Introduction

The light-scattering technique originally proposed by Rosenweig (1959) has often been employed for measurement of particle concentration in turbulent flow fields. In an initial study, Rosenweig, Hottel & Williams (1961) investigated turbulent diffusion in a free jet. A later series of investigations by Becker, Hottel & Williams (1963, 1965, 1967*a*) focused on particle diffusion in a ducted turbulent jet. Other studies include turbulent dispersion in a pipe flow (Becker, Rosenweig & Gwozdz 1966), concentration fluctuations in a turbulent flame (Gurnitz 1966), mixing in a well-stirred reactor (Hottel, Williams & Miles 1967) and additional work on the free jet (Becker, Hottel & Williams 1967*b*).

The technique exploits the light-scattering property of small particles. As illustrated in figure 1, a portion of the turbulent flow is seeded with fine particles and illuminated with a collimated beam of light. When the concentration of particles is sufficiently small, the intensity of the scattered light reaching the detector is linearly related to the number of particles in the control volume. By careful attention to the geometry of the optical system, the control volume can be made small enough to be considered a 'point'. For the usual particle concentrations and incident light intensities, the flow is unaffected by the measurement.

All of the work cited was accomplished with systems employing conventional light sources. The capability of the technique with such a source has been discussed by Becker, Hottel & Williams (1967*c*). They reported that with the typical

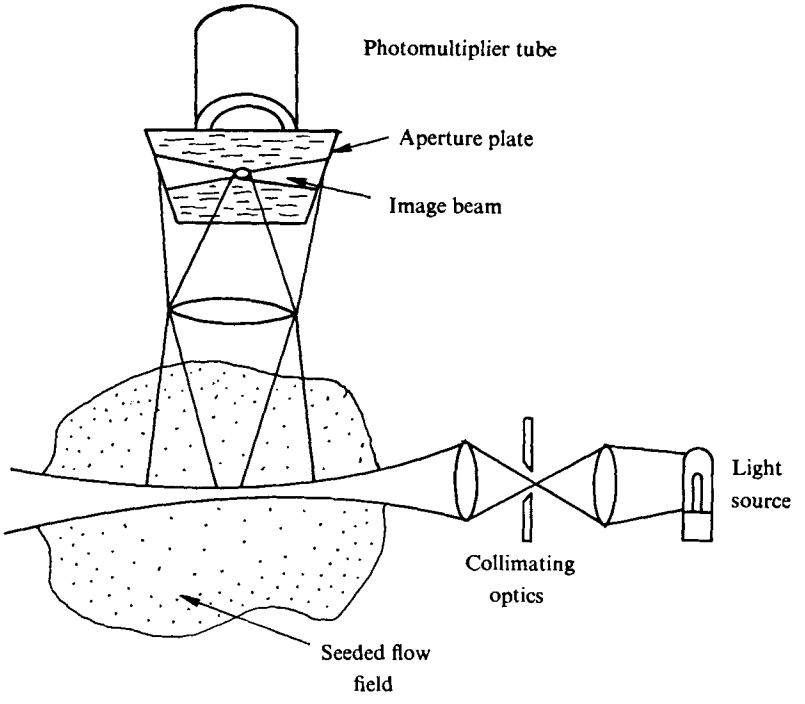

FIGURE 1. The light-scattering technique.

experimental arrangement the ultimate resolution of concentration fluctuations was limited by the detector's electronic shot noise level. If a more powerful light source were available, this level could be reduced. Becker *et al.* also discussed the influence of a 'marker' shot noise process on measurements of concentration fluctuations. This noise arises from the random arrival in the control volume of the particles which 'mark' the flow field. Owing to the high detector shot noise level in their system, Becker and his coworkers were unable to verify the presence of marker shot noise. This type of shot noise process was discussed by Lumley, George & Kobashi (1969) in the context of laser-Doppler velocimetry, and is usually referred to as ambiguity noise.

It is appropriate at this point to discuss the basic assumption that the intensity of scattered light reaching the photodetector is linearly related to the number of particles in the control volume. This is strictly true only for uniformly sized, identical particles under conditions of independent scattering. While the latter condition can be met by keeping the overall transmissivity sufficiently large (Van de Hulst 1957, chap. 1), it is quite difficult to achieve the former. The smoke generator employed here generates polydisperse particles. As a result, it is not possible to measure absolute number density at all. We suppose instead that the distribution of particle sizes is the same everywhere in the flow field at any instant. The intensity of the scattered light will then be proportional to a weighted (by size) average number density in the control volume. The particle concentration at any location can only be measured relative to the concentration at other locations. The validity of this approximation depends on the average number of

particles $\overline{N}$ in the control volume at every instant. When $\overline{N}$ becomes too small, we no longer have a large enough sample to characterize the distribution. This is precisely the condition, in fact, for which ambiguity noise becomes large. The usefulness of the technique depends on the existence of an average number density small enough for independent scattering to occur and large enough for the particle size distribution in the control volume to be the same everywhere at every instant.

The present work was motivated in part by a desire to explore the limitations imposed by ambiguity noise on the light-scattering technique. The flow field itself is one of obvious practical importance, and thus is well documented. The measurements reported here were made in the far field of a turbulent jet exhausting into a secondary air flow. Because of the high beam intensity of the argon-ion laser used as the light source, electronic shot noise was negligible. Ambiguity noise was detected, and found to be a fundamental limitation on spectral measurements. A theoretical estimate of the ambiguity noise spectrum and its dependence on the size of the control volume and the particle concentration is given. Some experimental results are presented which support these predictions. The capability of the present system for simultaneous velocity measurement using laser-Doppler techniques is currently being exploited for measurements of the velocity–concentration correlation.

2. Ambiguity noise

A complete discussion of the various noise sources which affect the laser light-scattering system is contained in Shaughnessy (1975). Most of these noise sources also affect a conventional light-scattering system and have been discussed in that context by Becker *et al.* (1967*c*). Here the intention is primarily to discuss ambiguity noise, which poses a fundamental limitation on the resolution of concentration fluctuations.

There are two other sources of noise, however, which deserve mention. Both are easily controlled by proper design of the laser light-scattering system. Electronic shot noise, which arises in the detector, is minimized by making the scattered light flux reaching the detector large, thereby reducing the gain required to produce a usable signal. Since the mean-square shot noise current is proportional to the gain squared, this is very effective. With the laser used here, electronic shot noise was never significant.

The second noise process is due to optical path attenuation. This noise is controlled by careful attention to the overall smoke concentration used to mark the jet. The presence of smoke particles along the optical path of the laser beam causes attenuation of the beam intensity through absorption and scatter. The same is true, of course, for the optical path from the control volume to the detector. It is easy to show that for a given path length the beam intensity decreases exponentially with the number of smoke particles along the path. When this number fluctuates in time, a complex modulation is added to the scattered light field and reaches the detector as noise. In the present work it was possible to adjust the smoke concentration such that this noise was less than 0·1 % of the

mean signal. During the course of this adjustment, the beam attenuation through the complete optical path was monitored. Experience shows that, when the mean beam attentuation is less than 5 %, the attenuation noise due to turbulent fluctuations in the particle content of the optical path is very small. If sufficient laser power is available to maintain the intensity of the scattered light field (and thus control detector shot noise) as the smoke concentration is reduced, it should be possible to minimize attenuation noise in most flows.

A rough analysis of attenuation noise proceeds as follows. Let τ be the transmissivity along the path and Q^* the extinction cross-section (cf. Shaughnessy 1975). Then

$$\tau = \exp\left[-Q^* \int_0^x \eta(x')\,dx'\right],$$

where η is the number of particles per unit volume along the path. The percentage extinction along the path is then defined as $1-\tau$. If we decompose η into

$$\eta(x) = \bar{\eta}(x) + \eta'(x),$$

where $\bar{\eta}(x)$ is the local average concentration and $\eta'(x)$ is the fluctuation from that average, then

$$\tau = \exp\left[-Q^* \int_0^x \bar{\eta}(x')\,dx'\right] \exp\left[-Q^* \int_0^x \eta'(x)\,dx'\right].$$

Assuming that the exponents are both small, τ may be approximated as

$$\tau \simeq \left(1 - Q^* \int_0^x \bar{\eta}(x')\,dx'\right)\left(1 - Q^* \int_0^x \eta'(x')\,dx'\right).$$

If $\tau = \bar{\tau} + \tau'$, then averaging this expression yields

$$\bar{\tau} = \left(1 - Q^* \int_0^x \bar{\eta}(x')\,dx'\right)$$

and

$$\tau' = -\bar{\tau} Q^* \int_0^x \eta'(x')\,dx'.$$

Thus the relative attenuation noise level squared is

$$\frac{\overline{\tau'^2}}{\bar{\tau}^2} = Q^{*2} \int_0^x \int_0^x \overline{\eta'(x'')\,\eta'(x')}\,dx'\,dx''.$$

As a rough approximation, this integral yields

$$\overline{\tau'^2}/\bar{\tau}^2 \simeq Q^{*2} \lambda^2 \overline{\eta'^2},$$

where λ is an average integral scale and $\overline{\eta'^2}$ the mean-square fluctuation.

Now if $\epsilon = 1 - \bar{\tau}$ is the percentage extinction across the jet, then $\epsilon \simeq Q^* L \eta^*$, where η^* is the average concentration across the jet and L is the jet width. With this estimate the previous expression can be written as

$$\frac{\overline{\tau'^2}}{\bar{\tau}^2} = \frac{\lambda^2}{L^2} \frac{\overline{\eta'^2}}{\eta^{*2}} \epsilon^2,$$

or, taking the square root,

$$\frac{(\overline{\tau'^2})^{\frac{1}{2}}}{\bar{\tau}} = \frac{\lambda}{L} \frac{(\overline{\eta'^2})^{\frac{1}{2}}}{\eta^*} \epsilon.$$

For this experiment $\lambda/L \simeq 0{\cdot}1$, $\overline{(\eta'^2)}^{\frac{1}{2}}/\eta^* \simeq 0{\cdot}5$ and $\epsilon \simeq 0{\cdot}05$. Thus the relative fluctuation in the amount of light transmitted through the jet is approximately

$$\overline{(\tau'^2)}^{\frac{1}{2}}/\bar{\tau} = 0{\cdot}0025.$$

The measured value was 0·001.

The source of ambiguity noise lies in the discrete nature of the smoke which is used to mark the mixing field. For example, consider laminar convection of a 'frozen' random distribution of smoke particles into the control volume. In analogy with a result obtained by Chandrasekhar (1943), the frequency of observation of N'' particles in the control volume will follow a Poisson distribution. The relative mean-square deviation from the average value N^* is accordingly

$$\langle (N''-N^*)^2\rangle/N^{*2} = N^{*-1}. \tag{1}$$

Since the light-scattering system counts the number of particles in the control volume, these fluctuations appear as a 'marker' shot noise or ambiguity noise in the detector output.

The fundamental limitation on the resolution of concentration fluctuations posed by ambiguity noise is evident in (1). Once the overall smoke concentration has been chosen to minimize noise due to optical path attenuation, a continuous reduction in the size of the control volume to obtain better spatial resolution represents a continuous reduction in N^*. Better spatial resolution therefore comes at the expense of increasing ambiguity noise.

In the presence of turbulence, the preceding analysis must obviously be modified. Let n be the difference between the instantaneous number of particles N and the average number of particles $\bar{N}$ in the control volume. This fluctuation consists of two contributions: one due to the discrete nature of the particles and one due to the turbulent inhomogeneities. Assuming that these contributions are independent, the following analysis applies. Let $\tilde{N}$ be the number of particles that would be present in the absence of marker shot noise. Then n^2 can be written as

$$n^2 = [(N-\tilde{N})+(\tilde{N}-\bar{N})]^2. \tag{2}$$

The first term represents fluctuations due to marker shot noise while the second term represents the turbulent contribution. Choosing a fixed value of the turbulent fluctuation $\tilde{N}-\bar{N}$ and assuming that $N-\tilde{N}$ follows a Poisson distribution, the ensemble-averaged mean-square fluctuation is

$$\langle n^2\rangle = \langle[(N-\tilde{N})+(\tilde{N}-\bar{N})]^2\rangle = \tilde{N}+\langle(\tilde{N}-\bar{N})^2\rangle. \tag{3}$$

Averaging now over the turbulent inhomogeneities, we have

$$\overline{\langle n^2\rangle} = \overline{(n^2)}_{\text{turb}}+\bar{N}, \tag{4}$$

a result first obtained by Rosenweig *et al.* (1961). Here $\overline{(n^2)}_{\text{turb}}$ denotes $\overline{\langle(\tilde{N}-\bar{N})^2\rangle}$. The contribution of ambiguity noise to the relative mean-square fluctuation is therefore

$$\overline{\langle(N-\tilde{N})^2\rangle}/\bar{N}^2 = \bar{N}^{-1}. \tag{5}$$

A simple experiment was run to confirm the result (5). A small control volume of $7{\cdot}85\times10^{-4}$ mm^3 was selected. Then the average particle number density was

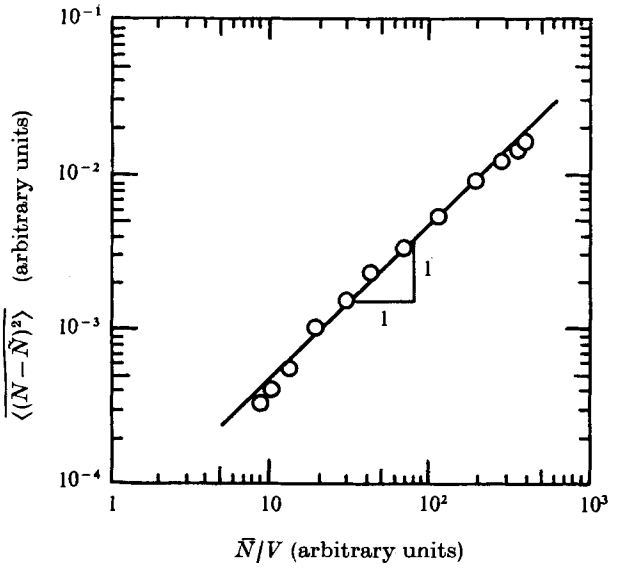

FIGURE 2. Effects of particle number density on ambiguity noise.

varied in steps over a range of one hundred times the initial density. At each particle density, the mean-square detector output in a fixed frequency band 10 kHz wide located at 80 kHz was measured. This ensured that only ambiguity noise contributed to the signal. After being corrected for electronic shot noise, the results were plotted in figure 2. The agreement with the predicted slope of + 1 is very satisfactory.

The spectral distribution of the ambiguity noise may be obtained in the following way. If the particles arrive in the control volume at a rate A in accordance with a Poisson process, then by Cambell's theorem (see Rice 1944) the autocorrelation function is given by

$$R(\tau) = \mathrm{A}\int_{-\infty}^{\infty} w(t)\, w(t+\tau)\, dt + \left[A\int_{-\infty}^{\infty} w(t)\, dt\right]^2, \tag{6}$$

where $w(t)$ is the detector response to a single particle. Following Lumley *et al.* (1969), an individual particle may be taken as producing a characteristic signal

$$w(t) = (S/2\pi)\exp[-t^2/2\sigma^2], \tag{7}$$

where the Gaussian form has been chosen because of the Gaussian intensity profile of the laser beam. Here S is the detector sensitivity to a single particle and σ is an arbitrary measure of beam width with time.

Using (7) in (6), the autocorrelation function for the fluctuations alone is

$$R(\tau) = \frac{AS^2}{2\sqrt{\pi}}\exp\left[\frac{-\tau^2}{4\sigma^2}\right]. \tag{8}$$

The power spectral density function as defined in Wax (1954) is

$$G(f) = 4\int_0^{\infty} R(\tau)\cos 2\pi f\tau\, d\tau, \tag{9}$$

D (mm)	f_D (Hz)	$f_{meas.}$ (Hz)
0·1	96192	180000
0·2	48092	80000
0·3	24048	48000
0·6	16032	33000

TABLE 1. Ambiguity noise frequency cut-offs.

where f is the frequency. For the ambiguity noise process described by (8) the spectral density is

$$G(f) = 2AS^2\sigma^2 \exp[-4\pi^2 f^2 \sigma^2]. \tag{10}$$

Let the diameter of the laser beam be defined by $d = \sigma\bar{U}$. The average rate at which particles enter the control volume is

$$A = (\bar{N}/V)\,\bar{U}dL, \tag{11}$$

where $\bar{N}$ is the average number of particles in a control volume of size V and L is the height of the control volume. Now for a cylindrical control volume V is simply $\frac{1}{4}\pi d^2 L$, hence $A = 4\bar{N}\bar{U}/\pi d$.

If D is the diameter of the laser beam at the $1/e^2$ point, it is easy to show that $d = \frac{1}{2}D$. With this substitution, the spectral density function becomes

$$G(f) = \frac{4S^2\bar{N}D}{\pi\bar{U}} \exp\left[\frac{-\pi^2 f^2 D^2}{\bar{U}^2}\right]. \tag{12}$$

The behaviour of this spectrum is flat for sufficiently small f, with

$$G(f_D) = e^{-1}G(0) \quad \text{at} \quad f_D = \bar{U}/\pi D.$$

The theoretical cut-off frequency is compared with the corresponding experimental value in table 1. The experimentally measured spectrum was analysed graphically to obtain a rough estimate of the cut-off frequency. As the results show, there is a consistent discrepancy in the magnitudes of the measured and theoretical cut-offs. This is not surprising considering the difficulty of measuring D with any accuracy. Here the value of D was assumed to correspond to the apparent edge of the beam as seen using a stereomicroscope with a calibrated eyepiece reticule. Though this measurement is not conclusive, the reasonable consistency of the table appears to support the suggested functional form of $G(f)$.

The overall effect of ambiguity noise on the concentration fluctuation power spectrum is shown in figure 3. The different curves correspond to various control-volume dimensions. Note that increases in spatial resolution result in increases in the ambiguity noise level. The spectra measured using the smaller control volumes are severely distorted.

The data in figure 3 were used to check the dependence of $G(f)$ on the beam diameter. For this purpose, $G(f)$ is normalized by the square of the mean detector output. The normalized spectrum is

$$G_n(f) = \frac{\pi D}{4\bar{U}(\bar{N}/V)\,V} \exp\left[\frac{-\pi^2 f^2 D^2}{\bar{U}^2}\right]. \tag{13}$$

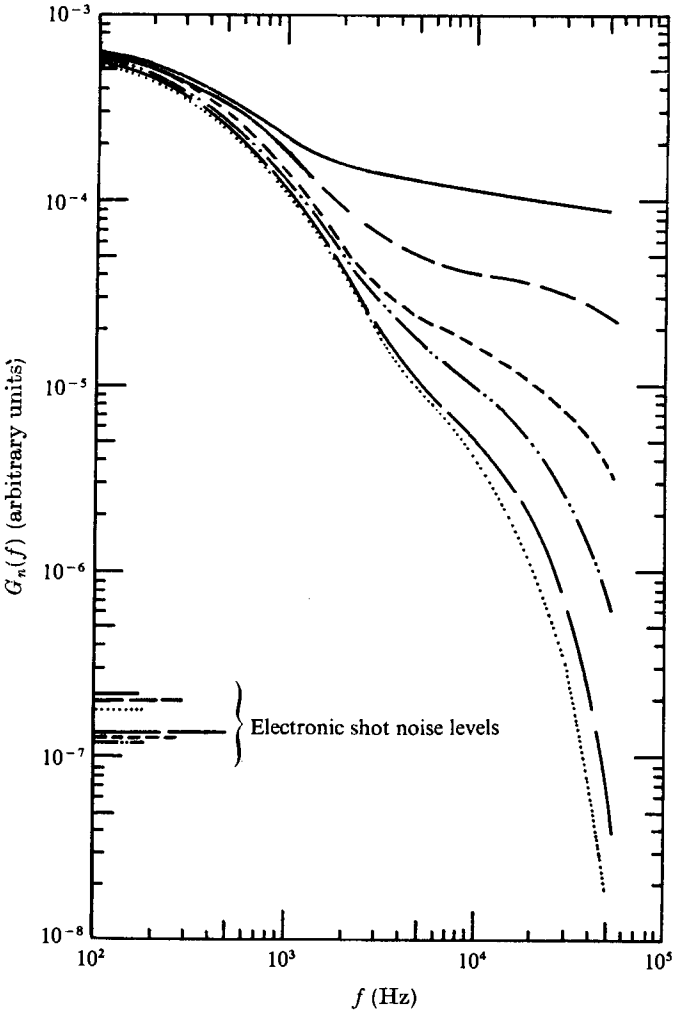

FIGURE 3. Ambiguity noise effects on the concentration fluctuation spectrum. Control volume (mm³): ·····, 0·785; ——·——, 0·402; —·—, 0·169; – – – – –, 0·150; ——·—·——, 0·00628; ——, 0·000785.

For a given frequency band centred at f, the amplitude of $G_n(f)$ is proportional to $D/V \propto D^{-2}$ since $V \propto D^3$ and $\bar{N}/V$ is the average fixed smoke concentration. Measurements of $G_n(f)$ taken at various frequencies in the range 20–30 kHz are plotted *vs.* the beam diameter in figure 4. The agreement between the measured points and a line of slope -2 is quite good. At the larger beam diameters departure from a -2 slope is expected since ambiguity noise no longer dominates the turbulence spectrum.

The conflicting requirements of low noise and good spatial resolution require a compromise in the design and operation of a laser-light-scattering system. In the present work, a beam diameter of 0·8 mm was chosen to control ambiguity noise. Noise due to optical path attenuation was minimized using the method described earlier. Sufficient laser power was always available to make electronic

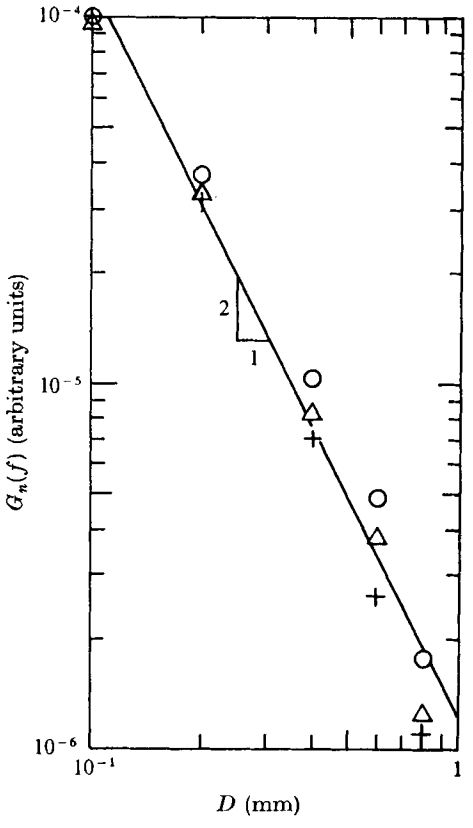

FIGURE 4. Dependence of spectral density on beam diameter.
Frequency (kHz): ○, 20; △, 25; +, 30.

shot noise completely negligible. Finally, it should be mentioned that the small overall dimensions of the present jet required much smaller control volumes than would be necessary with a larger facility. In larger flow fields ambiguity noise problems should be less severe.

3. Equipment and procedure

A Royco Model 258 Smoke Generator was used to produce a polydisperse dioctyl phthalate smoke with a mean particle size of $0{\cdot}3\,\mu$m. The output of the generator was diluted with large volumes of clean air and passed to the jet. The ratio of smoke to air was set to give a mean transmission of 95 % of the incident beam intensity. This ensured that noise due to optical path attenuation was negligibly small.

The jet was mounted on the centre-line of a low-speed wind tunnel. The diluted smoke entered the jet vertically through the hollow mount and left horizontally through a 6·35 mm round nozzle. The axis of the jet was parallel to the axis of the wind tunnel. To simplify traverse requirements the jet was mounted at various locations upstream of the fixed optical centre-line. Two air flow rates were used,

corresponding to Reynolds numbers based on the nozzle diameter of 56 052 and 31 590. Since little dependence of the measurements on Reynolds number was observed, no attempt has been made to present all the data taken at the lower Reynolds number.

The wind-tunnel test section is 215×305 mm in cross-section and 1 m long. A small constant-speed blower maintains a speed of 3·25 m/s in the test section and exhausts the tunnel to the atmosphere.

The optical system consists of the laser, focusing and collection optics, and a detector. A Spectra-Physics Model 165 argon-ion laser was employed as the light source. The beam intensity varied from 300 mW to as much as 2 W depending on the type of measurement. The power output was stable with a ripple of 1 % or less.

Focusing was accomplished with a simple lens. Beam diameters at the control volume were estimated by viewing the passage of the laser beam through an alignment jet 1 mm in diameter. An American Optical Company Model 750 Stereo microscope with a calibrated reticule was used to estimate the beam diameter.

The scattered light passed through a simple spatial filter operated at unit magnification, thereby allowing the length of the control volume to be determined by the diameter of standard pinhole apertures. The spatial filter was traversed by a modified Brinkman micromanipulator. Position repeatability proved to be excellent with this arrangement.

Most of the light detection was done with United Detector Technology Pin Silicon Photodiodes Models 020B and 040B. The diode output was amplified by a very low drift Philbrick amplifier with a gain of 10^3. The frequency response of the diode and amplifier was measured using a frequency-modulated laser and found to be flat beyond 20 kHz.

An EMI 9558C photomultiplier tube with an S-20 cathode was used as the detector for spectrum measurements. The tube was supplied with a direct current of 600–1000 V by a Keithley Instruments 246 High Voltage Supply. The frequency response of the photomultiplier tube extended well beyond 50 kHz.

A top view of the complete optical system is shown in figure 5. The laser head and mirror $M1$ are mounted on a large concrete pier. The beam passes through the focusing lens prior to entering the test section vertically. With the beam focused on the jet axis, radial traverses are achieved by moving the optical carrier along its track. As mentioned earlier, the jet is moved for streamwise traverses.

Mean signal voltages were measured using an integrator constructed from Philbrick operational amplifier elements. The integrator voltage was read with a Fluke 8000A Digital Multimeter. Root-mean-square voltages were measured with a DISA 55D35 r.m.s. voltmeter. Spectra were obtained in two ways: directly, using a Hewlett Packard 302A Wave Analyzer, and by numerically transforming autocorrelation curves produced by a Federal Scientific UC-202B Ubiquitous Correlator. The agreement was excellent.

Intermittency was measured by observing the presence of particles in the control volume. According to Becker *et al.* (1967*c*), the Schmidt number of micron-sized particles is about 4×10^4. Consequently, the boundary between the

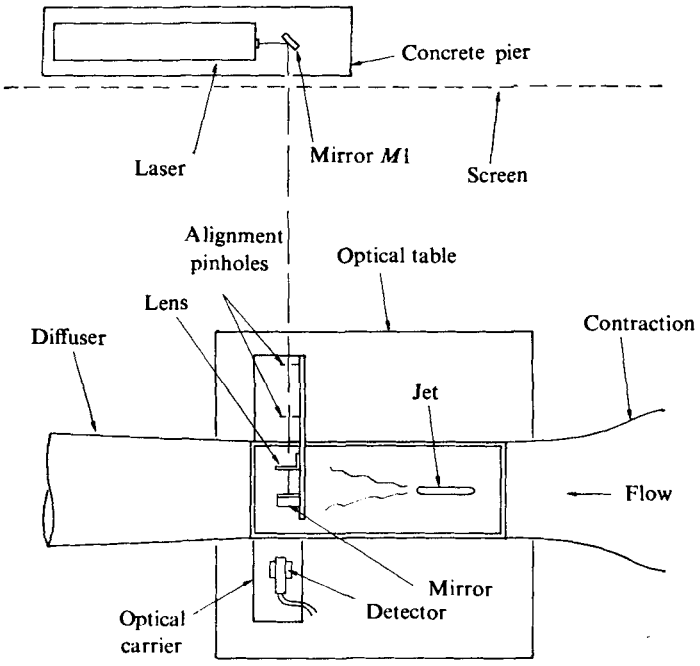

FIGURE 5. The optical system.

smoke-marked turbulent jet fluid and the clean secondary air flow was sharply defined. Assuming that the control volume is sufficiently small, the presence of particles in the control volume indicates that the flow is turbulent at that point. In the absence of noise, the intermittency is simply the fraction of time the concentration signal is non-zero. With noise present, the intermittency is equal to the fraction of time the concentration signal is greater than the noise level. The cumulative probability density of both the noise and the signal plus the noise was measured with the correlator. The intermittency was taken to be the fraction of time the detector output was above the voltage for which the noise cumulative density was 99 %.

The mean fluid velocity in the jet was determined using separate Pitot and static tubes of conventional design. Pressures were measured with a Datametrics Type 1012 Barocel Electric Manometer. The manometer output was time averaged and velocities were computed from the usual formula. No corrections were made for the effects of turbulence.

4. Experimental results

The notation used to present the data is shown in figure 6. The jet exhausts at velocity U_p from an orifice of diameter $2r_0$ into a uniform secondary stream of velocity U_s. At any location downstream, $\overline{U}_1$ is the mean velocity in excess of U_s. The half-width δ_v of the mean velocity profile is defined by $\overline{U}_1(\delta_v) = \frac{1}{2}\overline{U}_1(0)$. The mean concentration at any station is $\overline{\Gamma}$; the corresponding half-width is δ_c. The root-mean-square concentration fluctuation is γ.

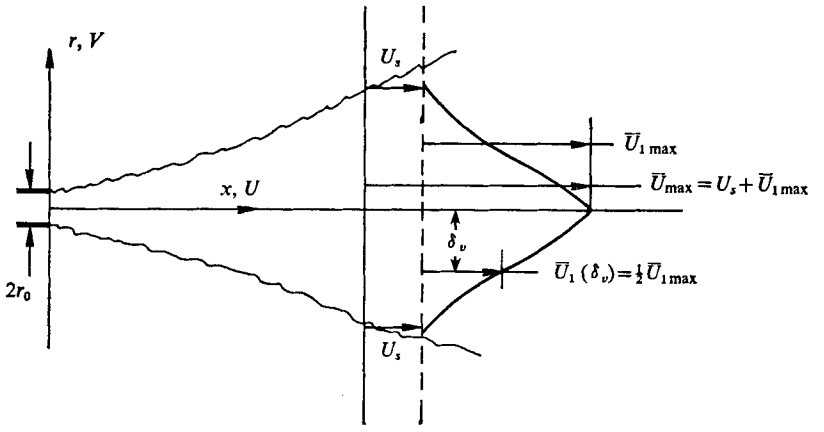

FIGURE 6. The turbulent jet.

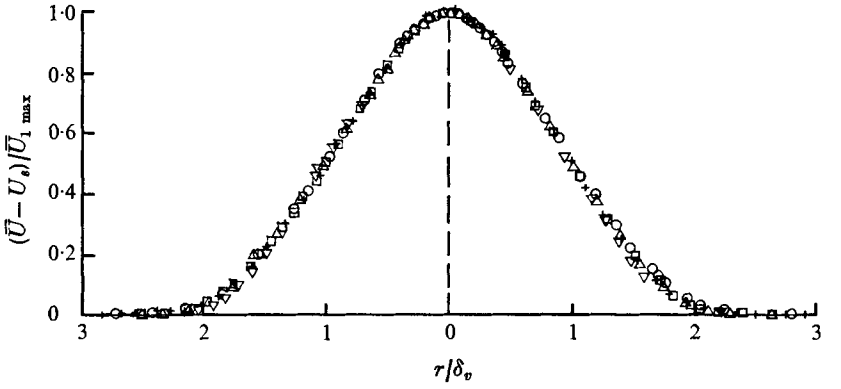

FIGURE 7. Mean velocity profile, $Re = 56052$.
$x/2r_0$: ○, 30; □, 40; △, 50; +, 70; ▽, 90.

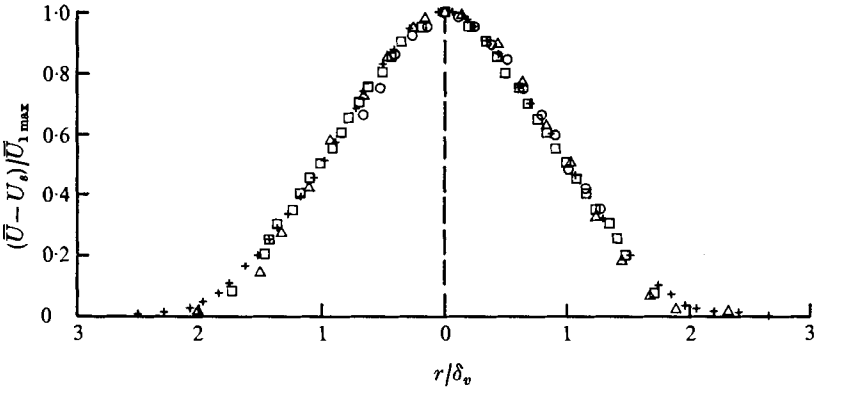

FIGURE 8. Mean velocity profile in turbulent jets. Source: +, present authors; ○, Gibson; □, Wygnanski & Fiedler; △, Antonia & Bilger.

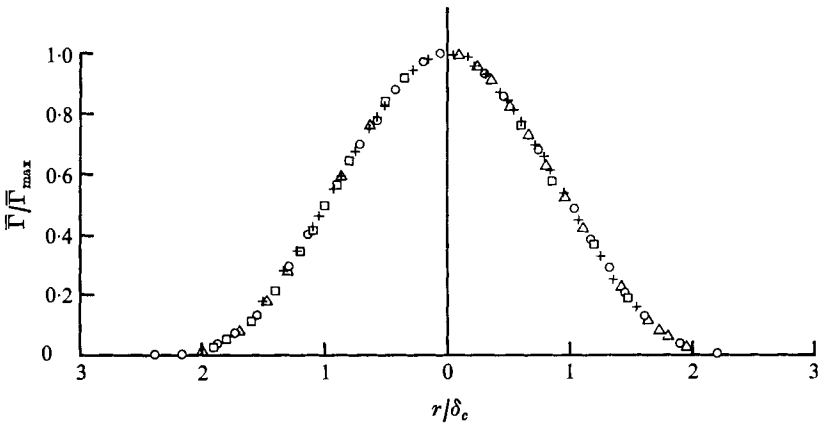

FIGURE 9. Mean concentration profile, $Re = 56052$.
$x/2r_0$: ○, 20; □, 30; △, 40; +, 50.

The profiles of mean velocity in the jet were found to be similar when normalized by $\overline{U}_{1\max}$ and δ_v. In the range $20 \leqslant x/2r_0 \leqslant 90$ these scales obeyed the power laws $\overline{U}_{1\max} \propto (x/2r_0)^{-1}$ and $\delta_v \propto x/2r_0$. The various concentration profiles were similar when non-dimensionalized using $\overline{\Gamma}_{\max}$ and δ_c. These scales behaved according to $\overline{\Gamma}_{\max} \propto (x/2r_0)^{-1}$ and $\delta_c \propto x/2r_0$.

The mean velocity profiles in the jet are shown in figure 7. Here the radial co-ordinate r is normalized by the local profile half-width δ_v. Figure 8 shows how the present profiles compare with those measured by Gibson (1963) and Wygnanski & Fiedler (1969) in free jets and also with data reported by Antonia & Bilger (1973) in a jet within a secondary air stream. In the latter arrangement the velocity ratio was $U_p/U_s = 3{\cdot}0$, compared with values of 24 and 42 for this work. The Reynolds numbers of the various jets shown in figure 8 are 5×10^4, 6×10^4 and $4{\cdot}6 \times 10^3$ respectively.

The mean concentration profiles at various locations along the axis of the jet are presented in figure 9. The collapse of the data onto a single profile demonstrates that the jet structure is similar. The present mean concentration data agree well with those measured using the conventional light-scattering technique. Figure 10 compares the present measurements with those taken by Becker *et al.* (1967*b*).

Figure 10 also shows the mean temperature profile reported by Corrsin (1943) for the heated free jet. The fact that the temperature and concentration profiles are substantially alike supports the suggestion of Hinze & van der Hegge Zijnen (1949) that there is little difference between the transport of heat and matter in the turbulent jet. A quantitative comparison of the transport of heat and smoke can be made on the basis of the values of the profile half-widths. These are shown in table 2. Here δ_T is the half-width of the temperature profiles reported by Corrsin (1943).

The measurements of Hinze & van der Hegge Zijnen (1949) as well as many others show that in the jet the spread of heat and matter is greater than that of momentum. This was true of the present data, as measured by the ratio δ_c/δ_v. Table 3 shows this ratio at various axial locations. For comparison purposes, this

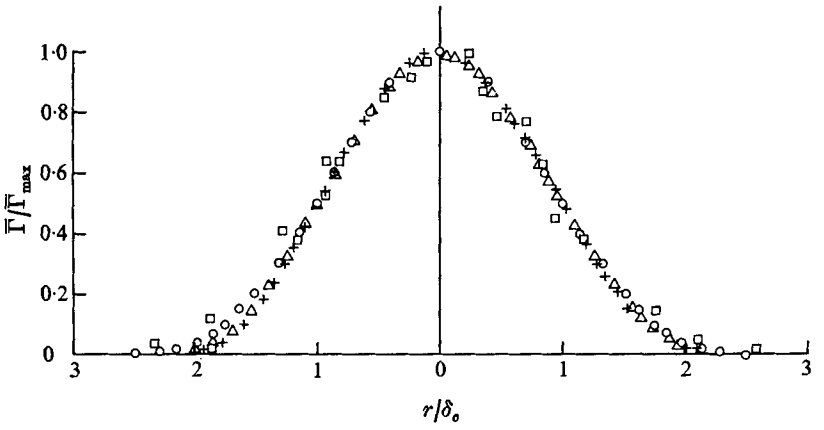

FIGURE 10. Mean admixture profiles in turbulent jets.
Source: △, +, present authors; □, Corrsin; ○, Becker *et al.* (1967*b*).

$x/2r_0$	$\delta_T/2r_0$	$\delta_c/2r_0$
20	2·28	2·17
30	3·43	3·17
40	4·65	4·15
50	—	5·36

TABLE 2. Comparison of admixture profile widths.

$x/2r_0$	δ_T/δ_v or δ_c/δ_v	Reference	Jet type
5	1·24	Corrsin (1943)	Heated, free, Re = 16700
10	1·42		
20	1·38		
30	1·38		
40	1·41		
15	1·25	Corrsin & Uberoi (1949)	Heated, free Re = 33000–67000
20	1·35		
30	1·18	Present authors	Smoke, confined Re = 56052
40	1·18		
50	1·26		
70	1·29		
30	1·16	Present authors	Smoke, confined, Re = 31590
40	1·20		
50	1·33		
70	1·44		

TABLE 3. Velocity and admixture profile half-width ratios.

ratio was also computed from data on the heated free jet reported by Corrsin (1943) and Corrsin & Uberoi (1949). The fact that the ratio δ_c/δ_v grows downstream is a clear indication that the present jet is not self-preserving.

The interesting finding by Forstall & Shapiro (1950) that the normalized profiles of mean velocity and admixture concentration in a turbulent jet were

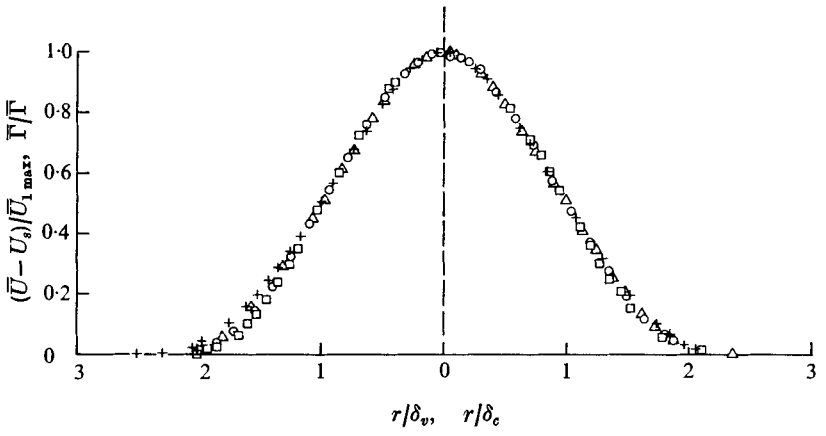

FIGURE 11. Similarity in the mean velocity and mean concentration profiles. ○, □, concentration, Re = 56052, 31590; +, △, velocity Re = 56052, 31590.

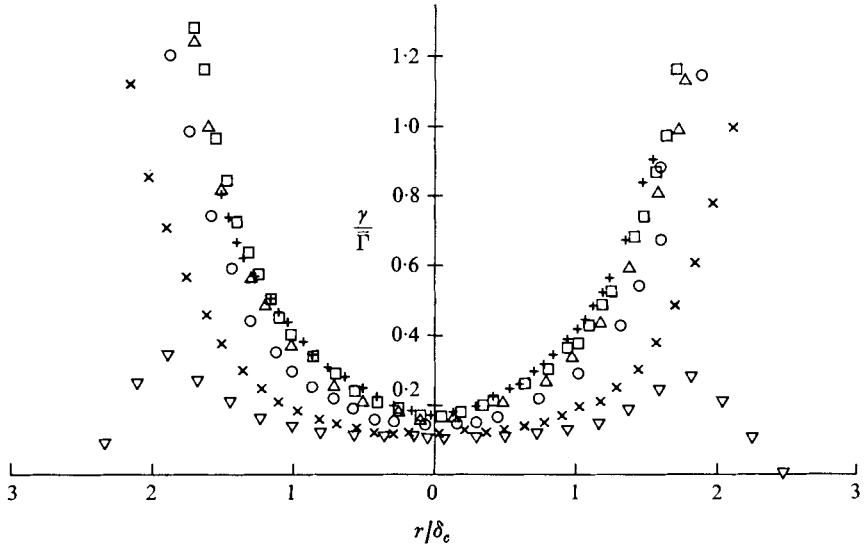

FIGURE 12. Concentration fluctuation profiles, Re = 56052. $x/2r_0$: ▽, 5; ×, 10; ○, 20; △, 30; □, 40; +, 50.

substantially alike was also checked. Their measurements were taken in a 10% by volume helium jet in a secondary air stream. Figure 11 shows a combined plot of the normalized mean velocity and mean concentration profiles. To check this suggestion further, the same curves were generated from the data of Corrsin (1943) and Corrsin & Uberoi (1949). These plots also supported this suggestion.

The concentration fluctuation profiles are shown in figure 12. Here the root-mean-square fluctuation has been normalized by the local mean concentration. Measurements in the outer region of the jet are complicated by the fact that the mean concentration rapidly falls to levels of the order of instrument noise while the fluctuations remain large. The occurrence of fluctuation intensities in the

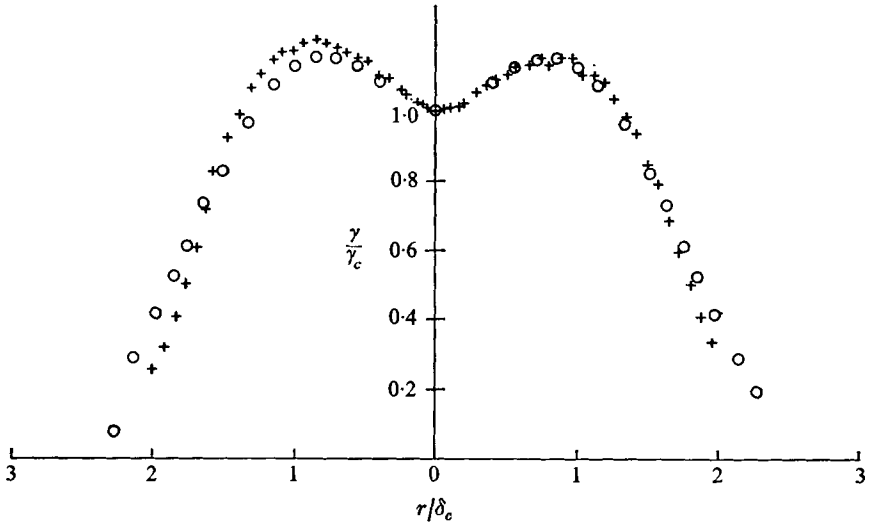

FIGURE 13. The self-preserving fluctuation profile.
Source: +, present authors; ○, Becker *et al.* (1967*b*).

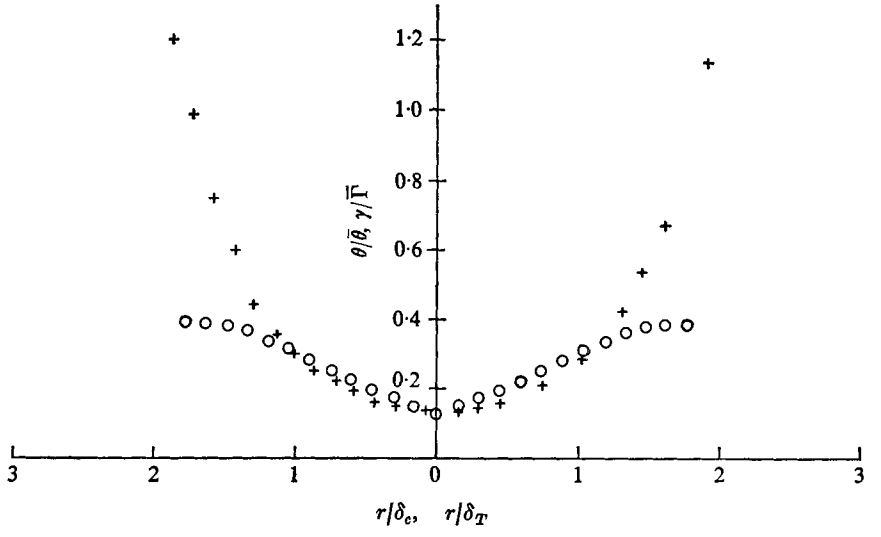

FIGURE 14. Admixture fluctuation profiles in turbulent jets, $x/2r_0 = 20$.
Source: +, present authors, ○; Corrsin & Uberoi (1949).

100 % range is evidence of the highly intermittent nature of the flow field in the outer region of the jet. The present measurements compare favourably with those taken by Becker *et al.* (1967*c*) using the conventional light-scattering technique. Plots of γ/γ_c obtained with the different light-scattering systems are shown in figure 13. Here γ_c is the centre-line root-mean-square concentration fluctuation. There is an obvious asymmetry in the present data, which apparently arises from an interference problem involving the wake of the jet mount. Otherwise the agreement is good.

Re	$x/2r_0$	$\delta_v/2r_0$	$\delta_c/2r_0$	$\delta_I/2r_0$
56052	20	—	2·17	3·31
	30	2·70	3·17	4·80
	40	3·52	4·15	6·30
	50	4·26	5·36	7·24
31590	20	—	2·08	2·99
	30	2·54	2·95	4·17
	40	3·21	3·84	5·51
	50	3·80	5·04	6·14

TABLE 4. Profile half-widths.

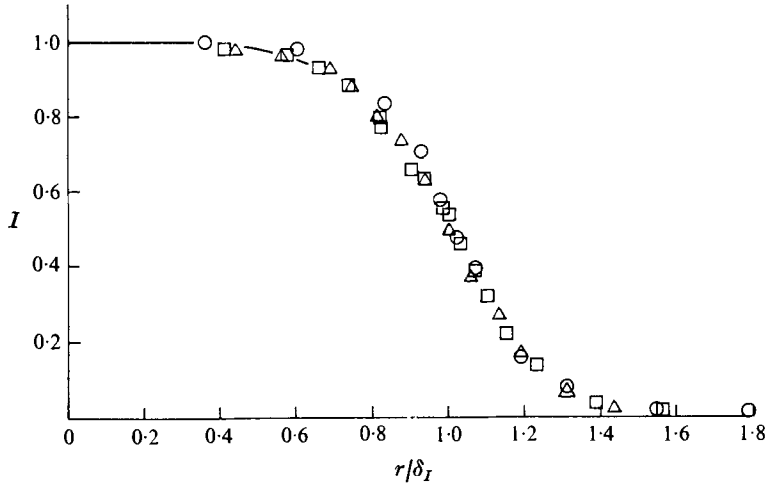

FIGURE 15. Intermittency distribution, $Re = 56052$.
$x/2r_0$: ○, 20; □, 30; △, 40.

Over most of the outer region of the jet the present fluctuation measurements differ considerably from those reported by Corrsin & Uberoi (1949). Their measurements of temperature fluctuations in a heated free jet indicate that a maximum fluctuation intensity of 0·4 is reached near $r/\delta_T = 1{\cdot}5$. Figure 14 compares the present results with theirs for $x/2r_0 = 20$. In view of the previously noted similarities in the transport of heat and smoke in the turbulent jet, it appears likely that instrument error is responsible. The reliability of a hot wire operated as a resistance thermometer in the high fluctuation environment of the outer portion of the turbulent jet has not been established.

Table 4 compares the measured intermittency profile half-width δ_I with the half-widths of the mean velocity and mean concentration profiles. The effect of Reynolds number is evident here. Although the normalized profiles do not exhibit noticeable Reynolds number dependence, this table indicates that the faster jet has a slightly stronger diffusive action.

Figure 15 is a plot of the intermittency distribution in the jet. As might be expected, the intermittency profile is strongly dependent on the size of the

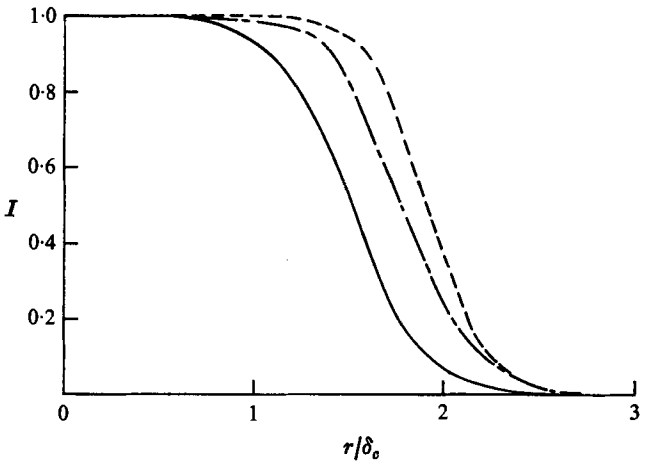

FIGURE 16. Self-preserving intermittency distribution, $x/2r_0 = 30$. Source: ——, present authors, $D = 0{\cdot}5$ mm; – – – –, present authors, $D = 1{\cdot}0$ mm; —·—, Becker *et al.* (1967*b*), $D = 0{\cdot}85$ mm.

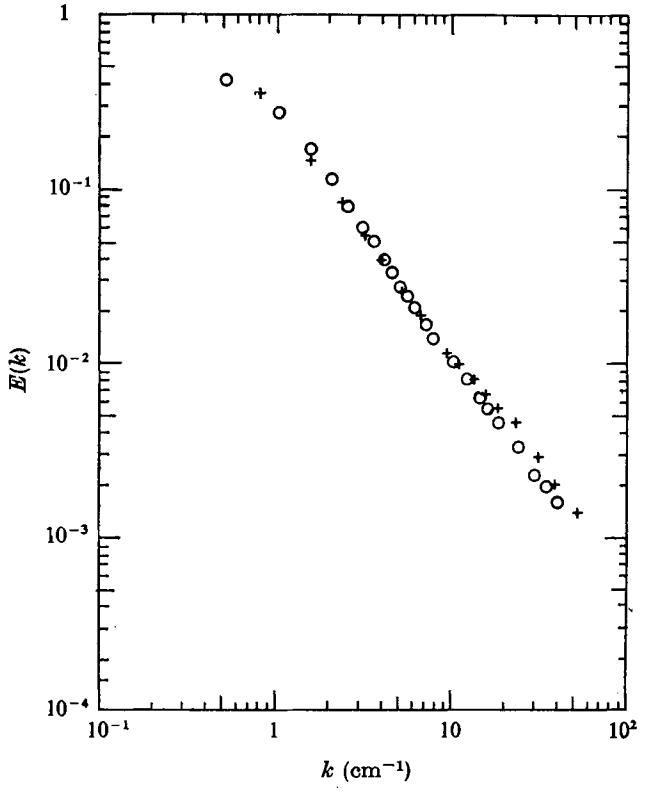

FIGURE 17. Concentration fluctuation spectrum, $Re = 56052$.
$x/2r_0$: ○, 30; +, 40.

Re	$x/2r_0$	$M/2r_0$	$I/2r_0$
56052	20	0·206	1·01
	30	0·246	1·50
	40	0·246	1·81
	50	0·241	2·26
	70	0·211	2·74
31590	20	0·195	1·02
	30	0·198	1·30
	40	0·200	1·63
	50	0·176	1·64
	70	0·162	2·04

TABLE 5. Micro- and integral scales; nozzle diameter $2r_0 = 6{\cdot}35$ mm.

control volume. A measure of this dependence can be seen in figure 16, demonstrating the sensitivity of this particular measurement to different control-volume sizes. While it is desirable to have good spatial resolution for this measurement, it is not obvious how small the control volume should be. If the control volume is made excessively small, ambiguity noise dominates, leading to errors in the intermittency. Similarly, if the control volume is excessively large, the intermittency will equal unity nearly everywhere. Thus there are restrictions on the possible volumes. The beam diameter of 0·5 mm used here was sufficiently small for the results to agree with the hot-wire survey of Wygnanski & Fiedler (1969).

The power spectrum of the concentration fluctuations was measured at several locations along the jet axis. These results, normalized to unit area, are shown in figure 17. The slight divergence of the curves at wavenumbers greater than 10 is believed to be due to ambiguity noise. As discussed in § 2, the ambiguity noise level is lower at $x/2r_0 = 30$ than at $x/2r_0 = 40$ owing to the lower velocity at the latter location.

There is little data available on the admixture fluctuation power spectra in jets. Becker *et al.* (1967*b*) used the conventional light-scattering technique in a free jet at approximately the same Reynolds number as here. After applying a correction for control-volume size they found that the high wavenumber region fitted a $-\frac{5}{3}$-power law. The present measurements, as well as those of Corrsin & Uberoi (1950), do not show this behaviour.

The concentration fluctuation microscales M and integral scales I along the jet centre-line are contained in table 5. These scales were computed from auto-correlation curves using Taylor's hypothesis. Though no data are available for comparison in the case of the microscales, the integral scales are in good agreement with those reported by Becker *et al.* (1967*b*). These measured integral scales are also consistent with the single measurement in the heated free jet reported by Corrsin & Uberoi (1950).

This work was supported by the National Science Foundation under grant GK 40126.

REFERENCES

ANTONIA, R. A. & BILGER, R. W. 1973 *J. Fluid Mech.* **61**, 805.

BECKER, H. A., HOTTEL, H. C. & WILLIAMS, G. C. 1963 *9th Symp. (Int.) Combustion*, p. 7.

BECKER, H. A., HOTTEL, H. C. & WILLIAMS, G. C. 1965 *10th Symp. (Int.) Combustion*, p. 1253.

BECKER, H. A., HOTTEL, H. C. & WILLIAMS, G. C. 1967*a* *11th Symp. (Int.) Combustion*, p. 791.

BECKER, H. A., HOTTEL, H. C. & WILLIAMS, G. C. 1967*b* *J. Fluid Mech.* **30**, 285.

BECKER, H. A., HOTTEL, H. C. & WILLIAMS, G. C. 1967*c* *J. Fluid Mech.* **30**, 259.

BECKER, H. A., ROSENWEIG, R. E. & GWOZDZ, J. R. 1966 *A.I.Ch.E. J.* **12**, 964.

CHANDRASEKHAR, S. 1943 *Rev. Mod. Phys.* **15**, 1–89.

CORRSIN, S. 1943 *N.A.C.A. Wartime Rep.* W-94.

CORRSIN, S. & UBEROI, M. 1949 *N.A.C.A. Tech. Note*, no. 1865.

CORRSIN, S. & UBEROI, M. 1950 *N.A.C.A. Tech. Note*, no. 2124.

FORSTALL, W. & SHAPIRO, A. H. 1950 *J. Appl. Mech.* **17**, 399–408.

GIBSON, M. 1963 *J. Fluid Mech.* **15**, 161.

GURNITZ, R. N. 1966 Sc.D. dissertation, Massachusetts Institute of Technology.

HINZE, J. O. & VAN DER HEGGE ZIJNEN, B. G. 1949 *Appl. Sci. Res.* A **1**, 435.

HOTTEL, H. C., WILLIAMS, G. C. & MILES, G. A. 1967 *11th Symp. (Int.) Combustion*, p. 771.

LUMLEY, J. L., GEORGE, W. K. & KOBASHI, Y. 1969 *Proc. Symp. Turbulence Measurements in Liquids*, p. 3.

RICE, S. O. 1944 *Bell System. Tech. J.* **23**, 5.

ROSENWEIG, R. E. 1959 Sc.D. dissertation, Massachusetts Institute of Technology.

ROSENWEIG, R. E., HOTTEL, H. C. & WILLIAMS, G. C. 1961 *Chem. Engng Sci.* **15**, 111.

SHAUGHNESSY, E. J. 1975 Ph.D. dissertation, University of Virginia.

VAN DE HULST, H. C. 1957 *Light Scattering by Small Particles*. Wiley.

WAX, N. 1954 *Selected Papers on Noise and Stochastic Processes*. Dover.

WYGNANSKI, I. & FIEDLER, H. 1969 *J. Fluid Mech.* **38**, 577.